http://dx.doi.org/10.5012/bkcs.2012.33.8.2508

Purification and Structural Characterization of Cold Shock Protein from *Listeria monocytogenes*

Juho Lee, Ki-Woong Jeong, and Yangmee Kim*

Department of Bioscience and Biotechnology, Bio/Molecular Informatics Center, Konkuk University, Seoul 143-701, Korea
**E-mail: ymkim@konkuk.ac.kr*
Received April 5, 2012, Accepted April 30, 2012

Cold shock proteins (CSPs) are a family of proteins induced at low temperatures. CSPs bind to single-stranded nucleic acids through the ribonucleoprotein 1 and 2 (RNP 1 and 2) binding motifs. CSPs play an essential role in cold adaptation by regulating transcription and translation *via* molecular chaperones. The solution nuclear magnetic resonance (NMR) or X-ray crystal structures of several CSPs from various microorganisms have been determined, but structural characteristics of psychrophilic CSPs have not been studied. Therefore, we optimized the purification process to obtain highly pure *Lm*-Csp and determined the three-dimensional structure model of *Lm*-Csp by comparative homology modeling using MODELLER on the basis of the solution NMR structure of *Bs*-CspB. *Lm*-Csp consists of a β-barrel structure, which includes antiparallel β strands (G4-N10, F15-I18, V26-H29, A46-D50, and P58-Q64). The template protein, *Bs*-CspB, shares a similar β sheet structure and an identical chain fold to *Lm*-Csp. However, the sheets in *Lm*-Csp were much shorter than those of *Bs*-CspB. The *Lm*-Csp side chains, E2 and R20 form a salt bridge, thus, stabilizing the *Lm*-Csp structure. To evaluate the contribution of this ionic interaction as well as that of the hydrophobic patch on protein stability, we investigated the secondary structures of wild type and mutant protein (W8, F15, and R20) of *Lm*-Csp using circular dichroism (CD) spectroscopy. The results showed that solvent-exposed aromatic side chains as well as residues participating in ionic interactions are very important for structural stability. Further studies on the three-dimensional structure and dynamics of *Lm*-Csp using NMR spectroscopy are required.

Key Words : Cold shock protein, *Listeria monocytogenes*, Homology modeling, Purification, Structure

Introduction

Cold stress results in the expression of several proteins, including NusA (transcription factor), IF2 (initiation factor), L7/L12 and S6 (ribosomal proteins), ribosome-binding factor (RbfA), prolyl isomerase (PPiB), and predominantly, cold shock proteins (CSPs).[1] CSPs function as chaperones in response to cold shock and have been identified in a wide range of gram-positive and gram-negative bacteria, often present as 3 (as in *Bacillus subtilis*) to 9 (as in *Escherichia coli*) highly homologous members. Recently, CSPs were also found in *Aquifex aeolicus* and *Thermotoga maritima*, indicating that CSPs were present at the time of bacterial divergence, and therefore, are presumably an evolutionarily dated class of proteins.[2]

CSPs stimulate transcription of cold shock-inducible genes, translation initiation, and destabilization of non-productive secondary single-stranded nucleic acids by binding these nucleic acids with micromolar to nanomolar affinity. Destabilization takes places during anti-termination, inducing expression of various cold shock genes at low temperatures. Thus, CSPs act as nucleic acids chaperones, aiding protein synthesis and antiterminators of cold-induced genes. Although CSPs bind to Y-box sequences, which contain an inverted CCAAT box, with high affinity, binding experiments involving oligonucleotides have shown that both *E. coli* cold shock protein A (*Ec*-CspA) and *B. subtilis* cold shock protein B (*Bc*-CspB) preferentially bind to pyrimidine-rich oligonucleotides.[3,4] Binding to the Y-box sequence, either alone or in combination with poly thymine (T), was negligible[5,6]; CSPs bind with the highest affinities for (T)- or uracil (U)-rich sequences.[7]

Structures of *Bs*-CspB, *Ec*-CspA, and cold shock proteins from *Bacillus caldoyticus* (*Bc*-Csp) and *T. martima* (*Tm*-Csp) have been determined using X-ray crystallography and nuclear magnetic resonance (NMR) spectroscopy, respectively.[8-10] CSPs consist of a Greek key β-barrel structure, which includes 5 antiparallel β strands and an oligonucleotide/oligosaccharide binding (OB) fold. The OB fold includes 2 conserved sequence motifs, ribonucleoprotein 1 and 2 (RNP 1 and 2). Many aromatic side chains are part of RNP 1 and 2.

Listeria monocytogenes is the causative agent of listeriosis, a disease that primarily affects pregnant women and their neonates as well as patients who are immunocompromised.[11] In the 1980s, several outbreaks of listeriosis were shown to be caused by the consumption of contaminated food. The range of temperatures over which *L. monocytogenes* can grow, 2-45 °C, is unusual for a pathogenic bacterium.[12] Thus, this organism is a fatal foodborne pathogen, which is viable at low temperatures because of the presence of CSPs.

In this study, *L. monocytogenes* cold shock protein (*Lm*-Csp) was cloned, expressed, and purified.[13] The three-di-

mensional structure model of *Lm*-Csp was determined using comparative homology modeling based on the solution NMR structure of *Bs*-CspB, and residues contributing to structural stability were analyzed. *Lm*-Csp variant proteins were successfully cloned and purified, and protein folding was evaluated using circular dichroism (CD) spectroscopy. This study provides insights into the structure and dynamics of *Lm*-Csp and contributes to the understanding of cold-shock adaptations in *L. monocytogenes*.

Methods

Construction of the *Lm*-Csp Expression Plasmid. To produce *Lm*-Csp in *E. coli* BL21 (DE3) cells, we cloned the *Lm*-Csp gene into the pET-11a expression vector containing an isopropyl-β-D-thiogalactopyranoside (IPTG)-inducible promoter and resistance to the antibiotic ampicillin with restriction enzyme, BamHI and NdeI. Polymerase chain reaction (PCR) was performed under the following conditions: 35 cycles of denaturation for 1 min at 94 °C, annealing for 1 min at 55 °C, and extension for 1 min at 72 °C. The *Lm*-Csp/pET-11a plasmid was transformed into expression cells, *E. coli* BL21 (DE3) cells, for expression of *Lm*-Csp.[14]

Site-Directed Mutagenesis. Construction of *Lm*-Csp variant plasmids with mutations at positions 8 (W8A), 15 (F15A), and 20 (R20A) were cloned using synthetic oligonucleotide primers (W8A forward primer 5'- GGT ACA GTA AAA GCG TTT AAC GCA GAA AAA - 3' and reverse primer 5' - TTT TCT GCG TTA AAC GCT TTT ACT GTA CCT - 3', F15A forward primer 5' - GCA GAA AAA GGA GCG GGT TTT ATC GAA CGC - 3' and reverse primer 5' GCG TTC GAT AAA ACC CGC TCC TTT TTC TGC - 3', and R20A forward primer 5' - GGT TTT ATC GAA GCG GAA AAC GGT GAC GAT - 3' and reverse primer 5' - ATC GTC ACC GTT TTC CGC TTC GAT AAA ACC - 3'). DNA used as the PCR template was extracted from *Lm*-Csp in *E. coli* BL21 (DE3) cells. Plasmid DNA was isolated using a standard alkaline lysis mini-prep method.[15] Template DNA (10 fmol) and primer sets (1 μM each) containing 0.2 mM of each dNTP and 2 μM Taq polymerase were amplified using PCR. Amplification was performed using the following PCR conditions: denaturation at 94 °C (1 min), annealing at 54 °C (1 min), and primer extension at 72 °C (1 min) for a total of 18 cycles. The variant *Lm*-Csp plasmid was transformed into *E. coli* BL21 (DE3) cells.

Expression of Wild-Type and Variant *Lm*-Csp. Transformed cells were grown on LB (Luria-Bertani) agar plates containing 50 μg/mL ampicillin. One colony was used to inoculate 50 mL of LB medium containing 50 μg/mL ampicillin. Cells grown overnight in at 37 °C. Next, 4 mL of the culture was mixed with 1 L of fresh LB medium containing 50 μg/mL ampicillin and grown until the optical density reached 0.8 at 600 nm. The culture was induced with 1 mM IPTG and was grown for 24 h at 10 °C, 15 °C and 20 °C to determine optimal *Lm*-Csp overexpression conditions. The cells were harvested and the cell pellet was stored at −72 °C.

Isolation and Purification of *Lm*-Csp. The frozen cell pellet was resuspended and lysed using ultrasonication in buffer A (6 mM Tris-HCl, 2 mM dithiothreitol [DTT], and 2 mM ethylendiamenetetraacetic acid [EDTA]; pH 6.8). After centrifugation at 16,000 rpm and 4 °C for 30 min, the supernatant was retained. The supernatant was loaded onto a Hitrap QFF column (anion exchange; GE) that had been preequilibrated with buffer A. The column was washed and bound protein was eluted using a linear gradient from 0 to 300 mM NaCl. The concentrated *Lm*-Csp-containing fraction was purified using size exclusion chromatography on a HiLoad 16/60 Superdex75 column (Parmasian) in size exclusion buffer (50 mM Tris-HCl and 100 mM KCl; pH 7.8). Finally, to optimize the purification conditions, hydrophobic interaction chromatography was performed using Resource reversed phase chromatography (RPC; GE). For this step, *Lm*-Csp containing fractions were purified either in potassium phosphate buffer or acetonitrile buffer to optimize purification conditions.

Circular Dichroism. CD experiments were performed using a J-810 (JASCO, Tokyo, Japan) spectropolarimeter with a 1-mm path length in the cell. CD spectra for *Lm*-Csp (50 mM) were recorded at 25 °C and 0.1 nm intervals from 190 to 250 nm (far-UV region). For each spectrum, data from 5 scans were averaged, and smoothed CD data were expressed as mean residue ellipticity (θ) in $deg \cdot cm^2 \cdot dmol^{-1}$.[16]

Comparative Protein Structure Modeling. The amino acid sequence of *Lm*-Csp comprised of 66 amino acids was retrieved from Expasy.[17] An *Lm*-Csp structure was constructed using comparative homology modeling on the basis of the solution NMR structure model of *Bs*-CspB. Sequence alignment of *Lm*-Csp with *Bs*-CspB (sequential identity, 75%) was conducted using the Insight/Homology module and adjusted to align key conserved residues. The structure model of *Bs*-CspB (Protein Data Bank [PDB] entry, 1NMF) was used as a structural template. Based on alignment results, 5 comparative models of the target sequence were built using MODELLER,[18] applying the default model-building routine 'model' with fast refinement. The energy function is a sum of many terms, including spatial restraints based on distributions of distances and dihedral angles in known protein structures. Energy minimization was performed using the consistent valence force field and Discover program using the steepest descent and conjugated gradient algorithms.[19]

Results and Discussion

Expression and Purification of Wild Type and Variant *Lm*-Csp. To optimize expression and purification conditions for *Lm*-Csp, cells were grown and induced at several temperatures. Various buffer conditions were used for purification based on purification protocols for *Colwellia psychrerythraea* (*Cp*-Csp) and *Bs*-Csp.[13] After inducing *Lm*-Csp expression at 3 different temperatures, 10 °C, 15 °C, and 20 °C, the cells were harvested and the cell pellet was stored at −72 °C. A temperature of 15 °C was determined to be the optimal growth temperature for *Lm*-Csp, because the highest expression of *Lm*-Csp was induced at this temperature. We

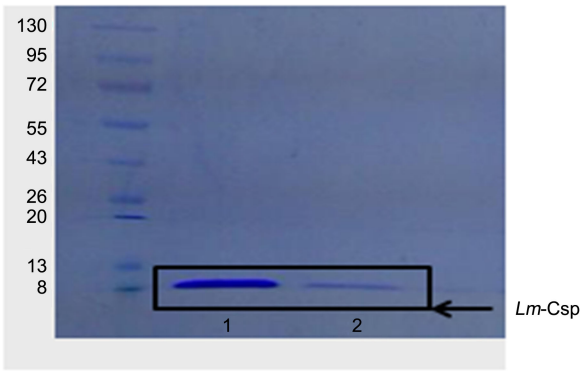

Figure 1. Purification of *Lm*-Csp produced from 1 L of LB medium as monitored by SDS-PAGE. The purified *Lm*-Csp showed a band corresponding to a molecular mass of 7.2 kDa. lane 1, result of a hydrophobic interaction chromatography purification with acetonitrile buffers; lane 2, result of potassium phosphate.

next determined optimized buffer conditions for hydrophobic interaction chromatography. In hydrophobic interaction chromatography, solvent exposed hydrophobic residues such as F15, F17, F27, F30 and F38 of *Lm*-Csp bind non polar stationary phase, implying that *Lm*-Csp has a folded structure. It was previously reported that *Bs*-CspB had been purified using potassium phosphate buffer and that *Cp*-Csp had been purified using acetonitrile buffer to obtain maximum yield.[13,22] Therefore, *Lm*-Csp was purified using the 2 different buffers using hydrophobic interaction chromatography. The dry weight yields of *Lm*-Csp using potassium phosphate and acetonitrile buffers were 0.2 mg/L and 1.0 mg/L in LB, respectively SDS-PAGE was applied to identify the *Lm*-Csp quantities in the each buffer and *Lm*-Csp was shown at a band corresponding to a molecular mass of 7.2 kDa (Figure 1). Compared to the yield of wild type *Lm*-Csp, yields of the variant *Lm*-Csp were 0.7 (W8A), 0.6 (F15A) and 0.7 (R20A) mg/L in LB media (Table 1), respectively.

Sequence Alignment. Amino acid sequences of *Lm*-Csp were aligned with those of other known CSPs, including *Tm*-Csp from *Thermotoga maritima*, *Bc*-Csp from *Bacillus caldolyticus*, and *Bs*-CspB from *Bacillus subtilis* (Figure 2). *Lm*-Csp showed sequence identity to *Tm*-Csp (58%), *Bc*-Csp (69%), and *Bs*-CspB (75%). Importantly, for *Tm*-Csp, *Bc*-Csp, *Bs*-CspB and *Lm*-Csp, amino acid sequences contain large numbers of aromatic residues, which are utilized for RNA binding. These aromatic residues are highly conserved in CSP family proteins. This protein family shares a cold shock domain (CSD) that contains the RNA-binding motifs RNP-1 and RNP-2. In mesophilic bacterium such as *Bs*-CspB, there are ionic interactions between K5 and E19, K7 and D25. Compared to *Bs*-CspB, more ion clusters are found additionally in thermophilic such as *Bc*-Csp and hyperthermophilic members such as *Tm*-Csp of the CSPs family. The side chains of arginine or lysine residues participate in a peripheral ion cluster and residues such as D20, R2, E47, and K63 are important for thermostability in *Tm*-Csp.[10] In *Lm*-Csp, E2 and R20 are the charged residues to form ion cluster.

Comparative Protein Structure Modeling. To determine a three-dimensional structural model of *Lm*-Csp and elucidate structural characteristics of *Lm*-Csp, 5 *Lm*-Csp models were generated using MODELLER. Energies and root-mean-square deviations (RMSDs) for 5 models are listed in Table 2. The average RMSD value for *Lm*-Csp compared with the template protein, *Bs*-CspB, was 1.61 Å and average energy was 261.83 kJ. Based on these data, the structure model of *Lm*-Csp is similar to that of *Bs*-CspB. Among the 5 *Lm*-Csp models, the lowest energy structure model was *Lm*-Csp 2, which is shown in Figure 3(c).

The structure model of *Lm*-Csp consists of 5 β strands, which form a Greek key β-barrel structure. These 5 β strands correspond to segments containing the residues G4-N10, F15-I18, V26-H29, A46-D50, and P58-Q64. Structural analysis of *Lm*-Csp revealed that *Lm*-Csp contains the RNP1 (K13-G14-F15-G16-F17-I18) and RNP2 (V26-F27-V28-H29-F30) sequence motifs commonly present in single-stranded nucleic acid binding proteins.[20,21] The RNP 1 and RNP 2 motifs are located on the same side of the *Lm*-Csp surface, supporting the hypothetical complex formation. Structure of complexes involving *Bs*-CspB and single-

Table 1. The yield of wild type and variant *Lm*-Csp in LB media

	Yield (mg/L)
Wild type	1.0
W8A	0.7
F15A	0.6
R20A	0.7

Table 2. RMSD and energy of 5 *Lm*-Csp models predicted using MODELLER

	RMSD with *Bs*-CspB (Å)	Energy (kJ)
Lm-Csp 1	1.63	271.26
Lm-Csp 2	1.61	240.42
Lm-Csp 3	1.66	260.28
Lm-Csp 4	1.54	270.19
Lm-Csp 5	1.62	266.98

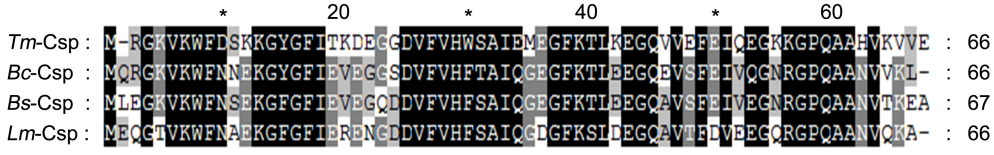

Figure 2. Sequence alignment for members of the cold shock protein (CSP) family, *Tm*-Csp, *Bc*-Csp, *Bs*-CspB (template protein), and *Lm*-Csp (target protein).

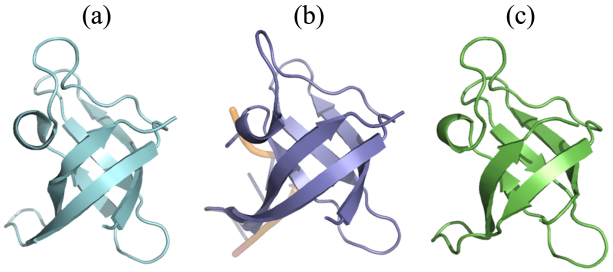

Figure 3. (a) Three-dimensional structure models of free *Bs*-CspB, (b) single-stranded nucleic acids bound to *Bs*-CspB, and (c) *Lm*-Csp.

stranded nucleic acids revealed that K7, W8, K13, F15, F17, F27, H29, F30, and R56 are involved in nucleic acid binding.[23] In *Lm*-Csp, these residues correspond to K7, W8, K13, F15, F17, F27, H29, F30, and R56. K13 and R56 are located in the loop regions on the surface of *Lm*-Csp. A comparison of the *Lm*-Csp structure with that of the template protein, *Bs*-CspB, and single stranded-nucleic acids bound to *Bs*-CspB is shown in Figure 3(a), (b), and (c). Similar folding patterns were observed for both proteins, while the surface loop structure of *Lm*-Csp differed between β strands β3 and β4 and between β4 and β5 compared to that of and *Bs*-CspB (Figure 4(a)). Particularly, the backbone conformations of loops β3-β4 of *Lm*-Csp were very different from those of *Bs*-CspB. Side-chain orientations of W8, F15, F17, and F27 involved in interactions with single-stranded nucleic acids are very similar for both proteins. It has been previously reported that aromatic residues contribute to the conformational stability of CSPs.[24]

In *Tm*-Csp, a single peripheral ion cluster around the side chains of R2 and D20 is important for thermal stability. These side chains are very close to each other. The distance from the side chain of R2 to the side chain of D20 in *Tm*-Csp is 3.4 Å, resulting in formation of a peripheral ion cluster.[10] The *Lm*-Csp structure model determined using comparative homology modeling revealed that E2 and R20 also form an

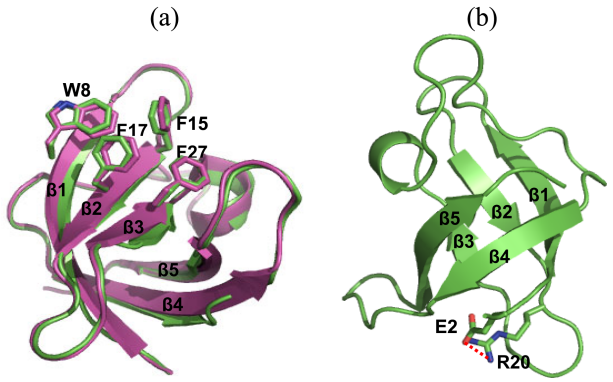

Figure 4. (a) Location of the characterized single-stranded nucleic acid binding epitope on the structure models of *Bs*-CspB (pink) and *Lm*-Csp (green). (b) *Lm*-Csp structure model (green). Side chain atoms of the basic residue R20 (blue) and the acidic residue E2 (red). The ionic interaction between R20 and E2 is shown in red dashed lines.

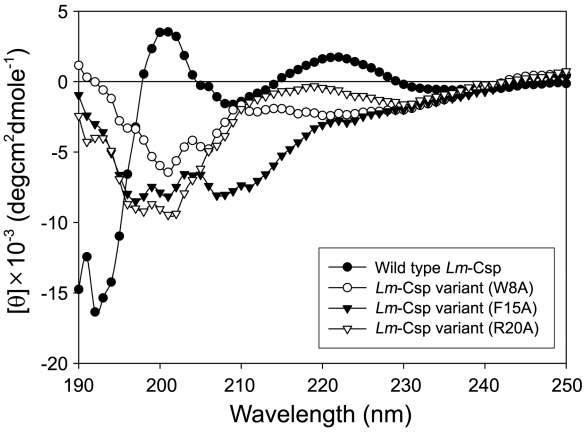

Figure 5. Circular dichroism (CD) spectra of wild-type *Lm*-Csp and its variants.

ion cluster, resulting in a distance of 3.0 Å from the side chain of E2 to the side chain of R20 (Figure 4(b)). This ionic interaction between E2 and R20 appears to be essential for *Lm*-Csp stability.

Circular Dichroism. CD spectra of wild-type and variant *Lm*-Csp are shown in Figure 5. Generally, a maximum positive band between 195-200 nm and a minimum negative band at 220 nm is characteristic of an antiparallel β sheet structure. CD spectra of CSPs reveal a predominantly β sheet structure. *Lm*-Csp contains 8 aromatic residues (7 Phe; 1 Trp). Aromatic side chains in properly folded proteins exhibit positive CD spectra between 215-230 nm.[25] Therefore, weak positive ellipticity between 215-230 nm has been attributed to aromatic side chains on the surface of β sheet as well as in the β sheet structure.[26-30] Between 195 and 205 nm, a CD maximum spectrum was observed due to the antiparallel β sheet structure of the protein.[31]

To examine the importance of exposed aromatic residues for RNA binding as well as the arginine residue for forming an ion cluster, we also investigated secondary structures of *Lm*-Csp variants, including W8A, F15A, and R20A, using CD spectroscopy. Compared to wild type *Lm*-Csp CD spectra, the *Lm*-Csp variant showed a negative band at 195-205 nm, implying that secondary structure of mutant proteins were changed and tertiary structure of variants were unfolded. Additionally, W8A and F15A showed negative bands between 215-230 nm, implying that regions near the aromatic residues had unfolded structures. Therefore, W8 and F15 as well as R20, which is important for forming ionic interactions, are important for conformational stability of *Lm*-Csp. The aromatic residues participate in *van der Waals* interactions between buried regions as well as in RNA binding. The R20 side chain appears to participate in an ionic interaction with E2 and plays a major role in the stability of *Lm*-Csp.

Conclusion

CSPs are a subgroup of cold-induced proteins preferentially expressed in bacteria and other organisms below standard physiological temperatures. These proteins are

related to the cold shock domain found in eukaryotes and represent some of the most highly conserved proteins known. Their exact functions remain unclear, but translational regulation, possibly *via* chaperoning of RNA, has been hypothesized based on three-dimensional structure models of several bacterial CSPs solved using NMR spectroscopy and X-ray crystallography.

In this study, we optimized expression and purification conditions, such as induction temperature and buffer conditions, for structural study. Optimal induction temperature was 15 °C, and *Lm*-Csp was successfully purified using acetonitrile buffer during hydrophobic interaction chromatography with high yield. Since structures of CSPs from psychrophilic bacteria have not been examined, the three-dimensional structure model of *Lm*-Csp was determined using comparative homology modeling with the solution structure of *Bs*-CspB used as a template protein. The *Lm*-Csp structure showed an OB fold consisting of 5 antiparallel β strands (G4-N10, F15-I18, V26-H29, A46-D50, and P58-Q64), which form a Greek key β-barrel structure. Compared to the template protein, *Bs*-CspB, *Lm*-Csp has a similar β sheet structure and an identical chain fold. Orientations of aromatic residues involving single-stranded nucleic acids interaction were similar to those of the *Bs*-CspB complex. However, *Lm*-Csp has shorter β sheet regions and more flexible structures than *Bs*-CspB.

We cloned, expressed, and purified 3 mutants of *Lm*-Csp, W8A, F15A, and R20A. Results of CD measurements showed that *Lm*-Csp has an antiparallel β sheet structure, while *Lm*-Csp variants such as W8A, F15A, and R20A, have unfolded structures. Thus, surface-exposed aromatic residues involving RNA binding and arginine residues participating in an ionic interaction are important for conformational stability of *Lm*-Csp. Further studies will investigate the three-dimensional structure and dynamics of *Lm*-Csp using NMR spectroscopy.

Acknowledgments. This work was supported by Konkuk University in 2011.

References

1. Graumann, P.; Schroder, K.; Schmid, R.; Marahiel, M. A. *J. Bacteriol.* **1996**, *178*, 4611-4619.
2. Phadatare, S.; Alsina, J.; Inouye, M. *Current Opinion in Microbiology* **1999**, *2*, 175-180.
3. Lopez, M. M.; Makhatadze G. I. *Biochem. Biophys. Acta* **2000**, *1479*, 196-202.
4. Lopez, M. M.; Yutani, K.; Makhatadze, G. I. *J. Biol. Chem.* **1999**, *274*, 33601-33608.
5. Lopez, M. M.; Yutani, K.; Makhatadze, G. I. *J. Biol. Chem.* **2001**, *276*, 15511-15518.
6. Zeeb, M.; Balbach, J. *Prot. Sci.* **2003**, *12*, 112-123.
7. Max, K. E. A.; Zeeb, M.; Bienert, R.; Balbach, J.; Heinemann, U. *FEBS Journal* **2007**, *274*, 1265-1279.
8. Max, K. E. A.; Zeeb, M.; Bienert, R.; Balbach, J.; Heinemann, U. *J. Mol. Biol.* **2006**, *360*, 702-714.
9. Delbruck, H.; Mueller, U.; Perl, D.; Schmid, F. X.; Heinemann, U. *J. Mol. Biol.* **2001**, *313*, 359-369.
10. Kremer, W.; Schuler, B.; Harrieder, S.; Geyer, M.; Gronwald, W.; Welker, C.; Jaenicke, R.; Kalbitzer, H. R. *Eur. J. Biochem.* **2001**, *268*, 2527-2539.
11. McLauchlin, J. *J. Appl. Bacteriol.* **1987**, *63*, 1-11.
12. Farber, J. M.; Peterkin, P. I. *Microbiol. Rev.* **1991**, *55*, 476-511.
13. Moon, C. H.; Jeong, K. W.; Kim, H. J.; Heo, Y. S.; Kim, Y. M. *Bull. Korean Chem. Soc.* **2009**, *30*, 2647-2650.
14. Jeong, K. W.; Lee, J. Y.; Kang, D. I.; Lee, J. U.; Hwang, Y. S.; Kim, Y. M. *Bull. Korean Chem. Soc.* **2008**, *29*, 1311-1314.
15. Birnboim, H. C.; Doly, J. *Nuc. Acids Res.* **1979**, *7*, 1413-1518.
16. Kim, W. H.; Back, S. H.; Kang, D. I.; Shin, H. C.; Kim, Y. M. *Bull. Korean Chem. Soc.* **2008**, *29*, 2259-2263.
17. Wilkins, M. R.; Gasteiger, E.; Bairoch, A.; Sanchez, J. C.; Williams, K. L.; Appel, R. D.; Hochstrasser, D. F. *Methods Mol. Biol.* **1999**, *112*, 531.
18. Marti-Renom, M. A.; Stuart, A.; Fiser, A.; Sanchez, R.; Melo, F.; Sali, A. *Annu. Rev. Biophys. Biomol. Struct.* **2000**, *29*, 291.
19. Lee, J. Y.; Kim, Y. M. *Bull. Korean Chem. Soc.* **2005**, *26*, 1695-1700.
20. Bandziluis, R. J.; Swanson, M. S.; Dreyfuss, G. *Genes Dev.* **1989**, *3*, 431-437.
21. Burd, C. G.; Dreyfuss, G. *Science* **1994**, *265*, 615-621.
22. Schindler, T.; Graumann, P. L.; Perl, D.; Ma, S.; Schmid, F. X.; Marahiel, M. A. *J. Biol. Chem.* **1999**, *274*, 3407-3413.
23. Zeeb, M.; Max, K. E. A.; Weininger, U.; Low, C.; Sticht, H.; Balbach, J. *Nucleic Acids Research* **2006**, *34*, 4561-4571.
24. Schindler, T.; Herrler, M.; Marahiel, M. A.; Schmid, F. X. *Nature Struct. Biol.* **1995**, *2*, 663-673.
25. Berova, N.; Nakanishi, K.; Woody, R. W. *Circular Dichroism*; Wiley-VCH: 2000; pp 612-614.
26. Woody, R. W. *Biopolymers* **1978**, *17*, 1451-1467.
27. Chakrabartty, A.; Kortemme, T.; Padmanabhan, S.; Baldwin, R. L. *Biochemistry* **1993**, *32*, 5560-5565.
28. Vuilleumier, S.; Sancho, J.; Loewenthal, R.; Fersht, A. R. *Biochemistry* **1993**, *32*, 10303-10313.
29. Sreerama, N.; Manning, M. C.; Powers, M. E.; Zhang, J. X.; Goldenberg, D. P.; Woody, R. W. *Biochemistry* **1993**, *38*, 10814-10822.
30. Sreeama, N.; Venyaminov, S. Y.; Woody, R. W. *Protein Sci.* **1999**, *8*, 370-380.
31. Perczel, A.; Park, K.; Fasman, G. D. *Proteins: Struct. Funct. Genet.* **1992**, *13*, 57-69.